International Journal of Mechanics and Energy (IJME)
Vol. 3, Issue 1, 2015, ISSN: 2286-5845

Transient modeling and simulation of an ammonia-water absorption solar refrigerator

Yasmina Boukhchana*, Ali Fellah, Ammar Ben Brahim

Research Unit: Applied Thermodynamics (UR:11ES80), National School of Engineers of Gabes (ENIG), University of Gabes, Omar Ibn El Khattab sreet, 6072 Gabes, TUNISIA

Abstract: The performance analysis of a solar absorption refrigerator operating in an autonomous way is investigated. The Ammonia/water machine satisfies the air-conditioning needs along the day. The refrigerator performances were simulated regarding a dynamic model. For the solar driven absorption machines, two applications could be distinguished. The sun provides the thermal part of the useful energy. In this case, it is necessary to use additional energy as the electric one to activate the pumps, the fans and the control system. On the other hand, the sun provides all the necessary energy. Here, both photovoltaic cells and thermal concentrators should be used. The simulation in dynamic regime of the cycle requires the knowledge of the geometric characteristics of every component as the exchange areas and the internal volumes. Real characteristics of a refrigerator available at the applied thermodynamic research unit (ATRU) at the engineers' national school of Gabes are notified. The development of the thermal and matter balances in every component of the cycle has permitted to simulate in dynamic regime the performances of a solar absorption refrigerator operating with the Ammonia/Water couple for air-conditioning needs. The developed model could be used to perform intermittent refrigeration cycle autonomously driven.

Key words: Solar Energy, Absorption refrigerator, Modeling, Simulation, Dynamic regime, Ammonia/Water.

1. Introduction

Recent environmental concerns on depletion of ozone layer and global warming have encouraged researchers to reconsider the absorption refrigeration systems, because of their friendliness with the environment [1, 2]. In the absorption systems, the mechanical process is replaced by a physico-chemical process since the compressor is eliminated. The system has low-work input requirement, and is also fairly simple and economical to operate. This is the superiority of these systems to the compression systems. As a result, low-grade energy such as solar, geothermal, and waste heat discharged from various industrial processes can be used as the input energy. The absorption systems reach the steady-state condition very fast, the dynamic analysis will be very important during the activation stage or part-load operation. Such a problem is extremely relevant for absorption chillers, where the high mass of the internal components and the accumulation of the fluids inside the vessels usually make the transient phase longer than in mechanical compression chillers. Dynamic simulation can also be applied for the controlling objectives of absorption systems.

Many papers have been published on the steady-state and dynamic simulation of absorption refrigeration systems [2-13]. Most of the existing attempts at dynamic absorption chiller modeling have resulted in the creation of detailed models of specific chillers or detailed models of specific cycles and system configurations [14, 15].

A computer simulation of a solar powered ammonia-water absorption cooling system with refrigerant storage was accomplished by Kaushik et al. [16]. The model required a known solution flow rate

***Corresponding author:** Yasmina Boukhchana
E-mail: Yasmina.Boukhchana@enig.rnu.tn.

as well as average hourly weather data and the cooling load patterns as input parameters. The design parameters of the system components were evaluated at rated conditions using the steady-state model. A dynamic model of the absorption refrigerator driven by hot water was developed by Sugano et al. [17] and was used as a tool for the design of a control system. To find suitable control strategies for an optimized operation of a double-lift ammonia-water chiller, a transient computational model using the software package TRANSYS was developed by Willers et al. [18]. A lumped-parameter dynamic simulation of a single-effect ammonia-water absorption chiller is performed by Kim et al. [14]. Modeling is based on the continuity of species constituting the ammonia-water mixture and the conservation of energy for each component of the absorption chiller. Ordinary differential equations governing the response of each component and the algebraic equations describing the constitutive relation are solved in parallel by numerical integration. The model has been applied to study the transients of temperature, pressure, concentration, and void fraction of each component during the start-up operation. The time constant of the absorption chiller is also investigated. In addition, the reduction of the time constant by a stepwise turn-up and turndown of the flue gas flow rate during the primary stage of start-up period is demonstrated. Other works have been recently presented by Boukhchana et al. [19, 20]; both works presented an effective dynamic model for the evaluation of temperature and concentration profiles of an intermittent solar absorption refrigeration system using NH_3/H_2O mixture. A dynamic model of a single-effect absorption refrigeration system using two different absorbent/refrigerant mixtures. (The first one is NH_3/H_2O and the second CO_2/bmimPF_6) was done by Cai et al. [21]. Modeling of the cycle performance requires thermodynamic properties which are obtained from an equation of state for the refrigerant-absorbent mixture. This study demonstrated that the COP of a system utilizing CO_2/bmimPF_6 is much lower than that of a traditional system using the NH_3/H_2O pair. The transient response of the cycle is investigated, and some design and operation parameters that affect the cycle performance are identified.

This present study has been planned with the aim to analysis, optimize and evaluate a transient response of a single-effect NH_3/H_2O absorption chiller. The ordinary differential equations deduced from mass and energy balances are solved using Runge-Kutta method. The results obtained from dynamic analysis are compared with those calculated based on steady-state approach and relative errors are reported.

2. Description of the system

A detailed flow diagram for the developed cycle is shown in Fig. 1. The water is chosen to be the heating fluid of the generator to ensure the least temperature and, consequently, concentration gradients along the height of the generator. The heating fluid is obtained from a solar collector. The heating process of the generator results in liberating ammonia–water vapour at a high pressure. This vapour is then passed through the condenser.

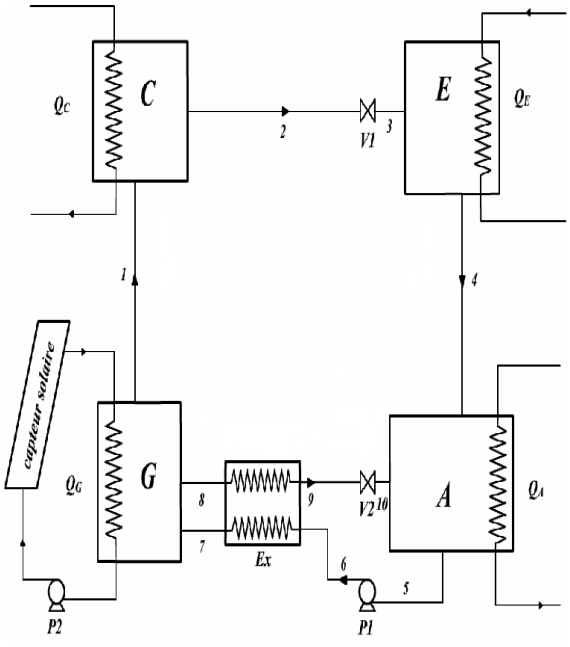

Fig. 1 Schematic of absorption refrigeration cycle.

The high pressure purified ammonia vapour is then condensed in an air-cooled condenser. This condensed ammonia is passed through an expansion valve which reduces its pressure and, consequently, its temperature to a lower value. The low temperature ammonia flows to the evaporator, which is installed under the ceiling of the cold room. Taking its latent heat of vaporization from the load stored in the cold room by natural convection, liquid ammonia vaporizes and flows to the absorber. Ammonia vapour is absorbed in the absorber by the weak solution coming in from the generator.

The strong solution is pumped from the absorber to the generator using a pump. A solution heat exchanger is incorporated to reduce the weak solution temperature before entering the absorber and to increase the temperature of the strong solution entering the generator. The temperature of the weak solution is decreased while flowing through an air-cooled weak solution secondary cooler, to decrease the absorber heat load and to increase the affinity of the weak solution to absorb the refrigerant. The weak solution is returned to the absorber via a throttling valve to maintain the pressure differential between the high and low sides of the system. The process proceeds until the desired temperature is achieved in the cold room.

Simple devices for regulating levels of liquid in the generator, the condenser and the evaporator are used to not enable draining of a component relative to another. The levels can be fixing by a level controller to control and adjust the fluid level, which explains the second current to the output of the condenser, the evaporator and the generator. In Fig. 2, a simple schematic of a level regulators and Fig. 3 showing it's mounting in an installation.

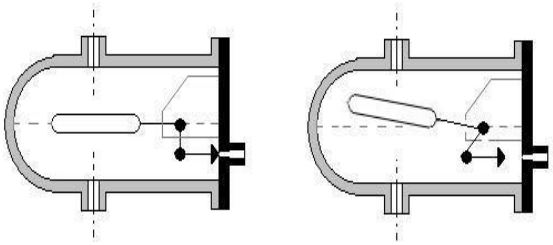

Fig. 2 Schematic diagram of a level controller.

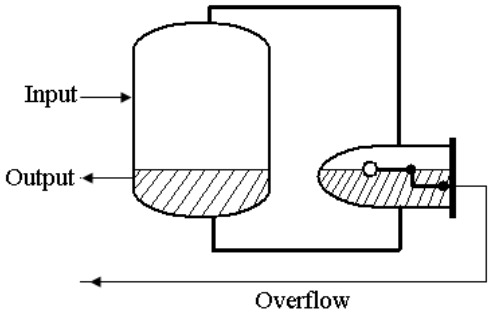

Fig. 3 Mounting of a level controller.

The transient simulation of cycle requires knowledge of the geometric characteristics of each component such as exchange area and internal volumes. The specifications of a refrigerator available at the applied thermodynamic research unit at the engineers' national school of Gabes are reported in Table 1 [22].

Table 1 Design parameters of the system

Element	Area (m^2)	Overall heat transfer coefficient ($kW\ m^{-2}\ K^{-1}$)	Internal volume (l)	Empty mass (Kg)
Generator	0.183	1.5	16.7	29.69
Absorber	0.8	0.7	15.1	10.25
Condenser	0.67	2.5	3.05	15.7
Evaporator	0.62	1.7	2.797	7.96

3. Formulation of dynamic model

3.1 Assumptions

In In the present study, in order to simplify the formulation and the consequent implementation of the model several conditions and assumptions were incorporated in the model without obscuring the basic

physical situation. These conditions and assumptions were as follows:

a. The power and thermal losses are ignored,
b. The expansion valves are supposed isenthalpic,
c. Only the expansion valves are responsible of the pressure variation,
d. Only pure frigorific fluid exists in the condenser and in the evaporator,
e. At the condenser's exit, the liquid is at a saturated state and temperature similar to prevailing in its interior,
f. At the evaporator's exit, the liquid is at a saturated state and temperature similar those prevailing in its interior,
g. At the absorber's exit, the rich solution is at the same temperature and concentration than those prevailing inside it,
h. At the generator's exit, the poor solution is at the same temperature and concentration than those prevailing inside it,
i. The solar collector components have the same exchange areas.

3.2 Dynamic model

3.2.1 Solar collector

The collector under consideration is a flat plat solar water collector. The functioning of this collector is described by the energy conservation equations written for all the components. The mathematical model obtained comprises four primary equation sets: (i) heat-balance equation of the glass cover; (ii) heat-balance equation of the absorber; (iii) heat-balance equation for heating fluid inside the collector; and (iv) heat-balance equation for heating fluid inside the generator.

The selected specification and design conditions of the solar collector are shown in Table 2.

(i). For the glass cover, the heat-balance equation is written as follows:

$$(MC)_C \frac{dT_C}{dt} = A.I.\alpha_C + A.\sigma.\varepsilon_C.\left(T_{Abs}^4 - T_C^4\right) + Ah_{Abs-C}\left(T_{Abs} - T_C\right) - A.\sigma.\varepsilon_C.\left(T_C^4 - T_{Ciel}^4\right) - Ah_{C-a}\left(T_C - T_a\right) \quad (1)$$

(ii). For the absorber the heat-balance equation is expressed as follows

$$(MC)_{Abs} \frac{dT_{Abs}}{dt} = A.I.\tau_C - A.\sigma.\varepsilon_C.\left(T_{Abs}^4 - T_C^4\right) - Ah_{Abs-C}\left(T_{Abs} - T_C\right) - Ah_{Abs-fl}\left(T_{Abs} - T_{fl}\right) \quad (2)$$

Table 2 Design parameters of the solar collector

Description	Parameter	Value
Area	A	12 m^2
Mass of glass cover	M_C	12 kg
Heat capacity of glass cover	C_C	0.02 $kJ.Kg^{-1}.K^{-1}$
Glass cover absorbance	α_C	0.06
Glass cover transmittance	τ_C	0.7
Emissivity	ε_C	0.15
Mass of the solar absorber	M_{Abs}	55.5 kg
Heat capacity of absorber	C_{Abs}	0.4 $kJ.Kg^{-1}.K^{-1}$
Mass flow rate of heating fluid	$\dot{m}_{fl}$	0.25 $kg.s^{-1}$
Heat capacity of heating fluid	C_{fl}, C_r	4.2 $kJ.Kg^{-1}.K^{-1}$
Mass of heating fluid in the absorber	M_{fl}	8.1 kg
Mass of heating fluid in the generator	M_r	10 kg

(iii). The heat-balance equation for heating fluid inside the collector and generator are given respectively by:

$$(MC)_{fl} \frac{dT_{fl}}{dt} = Ah_{Abs-fl}\left(T_{Abs} - T_{fl}\right) - Ah_{fl-a}\left(T_{fl} - T_a\right) - \dot{m}_{fl}.C_{fl}.\left(T_{fl}^{out} - T_{fl}^{in}\right) \quad (3)$$

Assuming that $T_{fl} \cong \frac{T_{fl}^{out} + T_{fl}^{in}}{1}$

$$(MC)_r \frac{dT_r}{dt} = \dot{m}_{fl}.C_{fl}.\left(T_{fl}^{out} - T_{fl}^{in}\right) A_r h_{r-a} (T_r - T_a) - U_G A_G (T_r - T_G) \quad (4)$$

3.2.2 Generator

The generator is modeled as a tubular heat exchanger. The rich solution is distributed at the bottom of the generator and rises in the tubes. The heating fluid flows outside the tubes, in the cylindrical shell, in counter-flow with ammonia-water mixture. The level in the generator is controlled by an overflow provided by the flow $\dot{m}_8^{'}$ through the auxiliary valve Vaux. When the liquid level in the generator is below a certain value, a level controller cancels the flow $\dot{m}_p$.

The basic mass, ammonia and energy balance equations for the generator are given as

$$\frac{dM_G}{dt} = \dot{m}_r + \dot{m}_2^{'} - \dot{m}_1 - \left(\dot{m}_p + \dot{m}_8^{'}\right) \quad (5a)$$

$$\frac{d\left(x_G M_G\right)}{dt} = x_r \dot{m}_r - x_p \left(\dot{m}_p + \dot{m}_8^{'}\right) \quad (5b)$$

$$\frac{d\left[M_G h_G + (MC)_G \left(T_G - T_{ref}\right)\right]}{dt} = Q_G + \dot{m}_r h_7 + \dot{m}_2^{'} h_2 - \dot{m}_1 h_1 - \left(m_P + m_8^{'}\right) h_8 \quad (5c)$$

Since $\dot{m}_r = \dot{m}_7$ et $\dot{m}_p = \dot{m}_8$

The heat responsible for the rise in the energy content in the generator derived from the solar collector is $Q_G = U_G A_G (T_r - T_G)$.

The steam leaving the generator approaches the equilibrium state corresponding to the temperature and pressure of the generator. As the residence time in the generator is insufficiently long for equilibrium conditions to be achieved, an approach to equilibrium is used for the calculation of the steam flow generated:

$$\dot{m}_1 = \dot{m}_r \frac{x_G^* - x_r}{x_G^*} \quad (6)$$

where x_G^* is the equilibrium concentration in the generator at the pressure and temperature of the generator.

3.2.3 Condenser

The condenser is modelled as heat exchanger coil where flows ammonia vapor and is condensed. This condensation is carried out by spraying the water at room temperature over the coil. In the condenser prevails a balance between the liquid and the vapor of the refrigerant (ammonia). High pressure is fixed by the temperature of the condenser: it's the vapor pressure at this temperature. Ammonia leaving the condenser is at the saturated liquid state.

The basic equations for the condenser are:

$$\frac{dM_C}{dt} = \dot{m}_1 - \dot{m}_2 - \dot{m}_2^{'} \quad (7a)$$

$$\frac{d\left[M_C h_C + (MC)_C \left(T_C - T_{ref}\right)\right]}{dt} = Q_C + \dot{m}_1 h_1 - \left(\dot{m}_2 - \dot{m}_2^{'}\right) h_2 \quad (7b)$$

We also know that the heat rejected by the condenser is $Q_C = U_C A_C (T_0 - T_C)$.

3.2.4 Evaporator

The evaporator is modelled as a coaxial heat exchanger (one inner tube and one outer tube). In the inner tube is water needs to be cooled. In the annular space, circulates the refrigerant which evaporates at a constant temperature corresponding to the low side pressure set by the equilibrium conditions in the absorber. The liquid level in the evaporator is controlled by an overflow through the flow $\dot{m}_4^{'}$. When the accumulation of liquid in the evaporator exceeds a

maximum level, it will be overturn entirety to the absorber. Furthermore, in the evaporator prevails a balance between the liquid vapor phase of the refrigerant

$$\frac{dM_E}{dt} = \dot{m}_3 - \dot{m}_4 - \dot{m}_4' \tag{8a}$$

$$\frac{d\left[M_E H_E + (MC)_E \left(T_E - T_{ref}\right)\right]}{dt} = Q_E + \dot{m}_3 h_3 - \dot{m}_4 h_4 - \dot{m}_4' h_4' \tag{8b}$$

Such as cooling capacity produced is

$$Q_E = U_E A_E \left(T_L - T_E\right)$$

For the calculation of the steam flow produced by the evaporator and absorbed in the absorber, it is assumed that the flow rate of the weak solution ($\dot{m}_p + \dot{m}_8'$) absorbs the steam flow $\dot{m}_4$ up to saturation at the temperature and pressure of the absorber.

$$\dot{m}_4 = \left(\dot{m}_p + m_8'\right)\frac{x_p - x_A^*}{x_A^*} \tag{9}$$

3.2.5 *Absorber*

The absorber is envisaged as a vertical shell and tube heat exchanger. The weak solution coming generator is distributed at the bottom and dissolves any refrigerant vapour coming from the evaporator. The water reduces the absorber temperature (by extracing the heat of mixing and heat of condensation of the refrigerant vapor) and improves the refrigerant solubility in the absorber. As equilibrium conditions are assumed to exist in the absorber, the low side pressure is that corresponding to the strong solution concentration and temperature of the absorber. The basic equations for the absorber are:

$$\frac{dM_A}{dt} = \dot{m}_4 + \dot{m}_4' + \dot{m}_p + \dot{m}_8' - \dot{m}_r \tag{10a}$$

$$\frac{d\left(x_A M_A\right)}{dt} = x_p\left(\dot{m}_4 + \dot{m}_8'\right) - x_r \dot{m}_r \tag{10b}$$

$$\frac{d\left[M_A H_A + (MC)_A \left(T_A - T_{ref}\right)\right]}{dt} = Q_A + \dot{m}_4 h_4 - \dot{m}_4' h_4' - \dot{m}_r h_5 + \left(\dot{m}_p + \dot{m}_8'\right) h_{10} \tag{10c}$$

3.2.6 *Heat Exchange*

This component is treated as a counter flow heat exchanger to have a constant efficiency. In other words transforms instantly the power of hot stream to the cold stream.

$$\dot{m}_r\left(h_7 - h_6\right) = \left(\dot{m}_p + \dot{m}_8'\right)\left(h_8 - h_9\right) \tag{11}$$

$$\varepsilon = \frac{T_8 - T_9}{T_8 - T_6} \tag{12}$$

3.2.7 *Pump*

Since the cycle is composed of two parts operating at different pressures, the fluid passage through these two parts requires the presence of a pump. This will ensure the transfer of the rich solution from the absorber to the heat exchanger.

$$\dot{m}_r = \frac{\eta_P \rho_r Q_P}{HP - BP} \tag{13}$$

$$Q_P = \dot{m}_r\left(h_6 - h_5\right) \tag{14}$$

3.2.8 *Expansion Valve*

The flows through the expansion valves are determined using a flow coefficient model. The model assumes the pressure differential across the valve as the driving force for the flow, and an adjustable section, A valve, represents the cross section of the expansion valve. This section will be taken of the conditions of steady.

$$\dot{m} = A_{valve}\sqrt{2.\rho.\left(HP - BP\right)} \tag{15}$$

3.2.9 Numerical implementation

Component models are created as re-usable blocks in the EES environment. The ordinary differential equations and other constitutive relations along with the property calls are solved in the EES environment for use predefined functions giving the thermodynamic properties of NH_3/H_2O mixture, and integrated using the Runge-Kutta algorithm. The time step for numerical integration is limited to a maximum of 0.05 s, and is automatically adjusted to satisfy the relative tolerance of 10^{-3} for the residuals of dependent variables.

4. Results and Discussion

The transient performance of the chiller is discussed in this section. The initial conditions and the operating conditions for the model are shown in Table 3.

Table 3 Selection of parameters

Parameter	Value
T_V^0, T_{Abs}^0, T_{fl}^0, T_r^0	20°C
T_G^0	20°C
T_A^0	30°C
T_C^0	30°C
T_E^0	20°C
M_G^0	20 kg
M_A^0	20 kg
M_C^0	0 kg
M_E^0	0 kg
x_G^0	48%
x_A^0	48%
T_0	30°C
T_L	5°C
ε	0.8

The glass covers temperature, the absorber temperature and the inside heating fluid temperature in the collector and generator of the collector calculated from the simulation model are shown in Fig. 4. It was found that the temperature of the absorber is the highest. This is explained by the absorption quality of the absorber. The primary function of the absorber plate is to absorb as much as possible of the radiation reaching through the glazing, to lose as little heat as possible upward to the atmosphere and downward through the back of the container, and to transfer the retained heat to the circulating fluid. Then, in a decreasing order, we have the temperature of the outlet water resulting from the convection coefficient between the absorber and the fluid. Afterwards the temperature of the air draped between the transparent cover and the absorber. Given the low absorption coefficient of the transparent cover (α_C = 0.02) and its affectation by the wind that causes heat loss by convection with ambient air the temperature variation of the glass cover is the lowest.

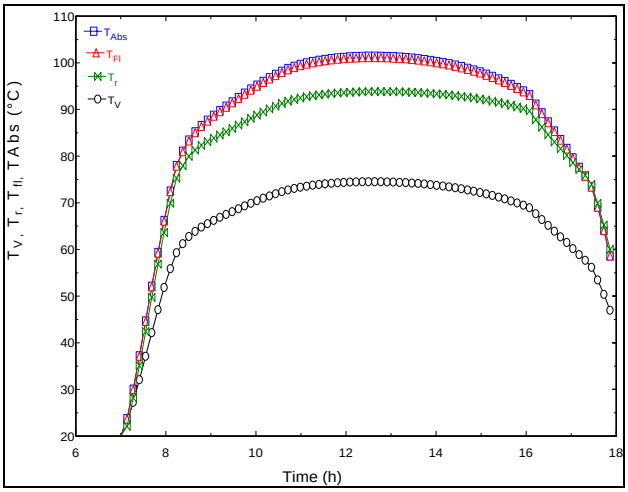

Fig. 4 Temperatures variations of the different components of the solar collector versus.

The components temperatures variations are represented in Fig. 5. The generator temperature T_G increases from 20°C to 90°C. Then, remains constant until 16h and it begins to decreases until 60°C. The condenser temperature T_C increases from 30°C to 35 °C, generating a pressure of 5.4 kPa in the high pressure compartment. The absorber's internal temperature increases from 30°C to 38°C. It remains constant and then it decreases. The evaporator internal

temperature stabilizes at 2°C. The low pressure of the machine is then 1.1 kPa.

The variations of the powers in the compartments of the machine are shown in Fig. 6. The stabilization of the power Q_E values in the evaporator and Q_A in the absorber is due to the stabilization of the internal temperatures of the components and of the flow rates m_4 and m'_4. The power Q_G absorbed by the generator increases as far as it reaches a maximal value of 6.2 kW toward 12.5 PM. The condenser power Q_C follows reverse variation than the power Q_G. The temperature in the generator increases then the steam flow rate produced increases and saturation conditions are achieved. The machine produces a 2.7 kW cooling load.

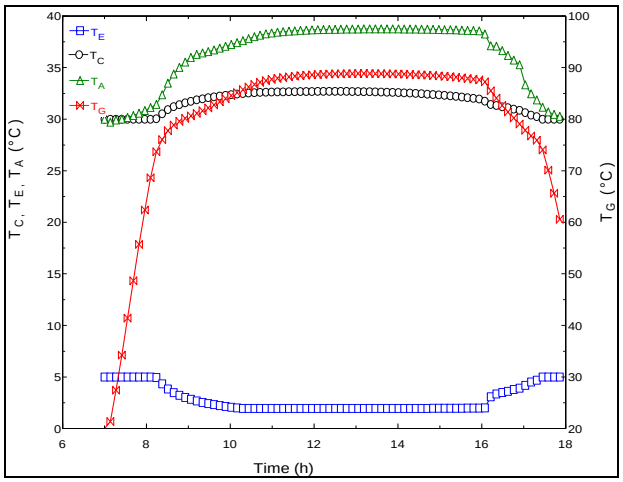

Fig. 5 System components temperatures as a function of time.

In Fig. 7 there is shown the variation with time of the rich solution flow (m_r), the poor solution flow (m_p), the flow of vapor desorbed in generator (m_1) and the steam flow absorbed by the absorber (m_4). It can be seen that the mass flows rates increase and the system quickly reaches a new steady state to 11 hr. The mass flow of rich solution reach 0.034 kg/s, then the poor solution reach 0.03 kg/s. The steam flow produced by the generator is larger than the flow rate absorbed at the absorber which is almost constant.

Fig. 8 represents the variations of the incidental and the generator powers as well as the variation of the solar collector efficiency according to the time. The average efficiency over the day is equal to 0.39.

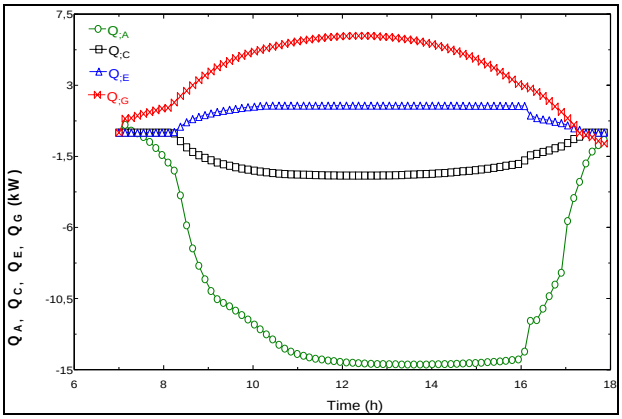

Fig. 6 Hourly rates of heat transfer in various components with time.

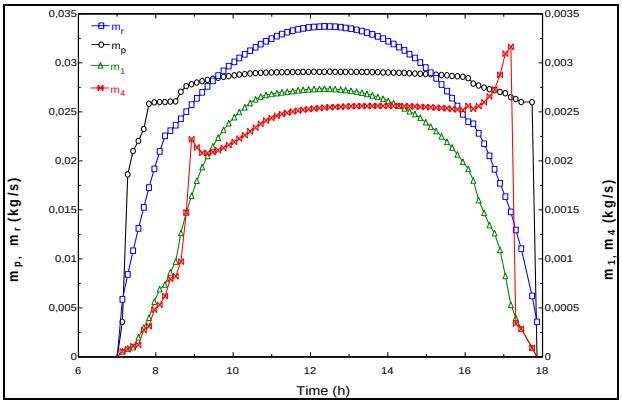

Fig. 7 Flows variation versus.

From the Fig. 9 it can be seen that the COP varies significantly from 9 hr to 16 hr. This variation is due to variation of the power absorbed by the generator because the power in the evaporator in this period is almost constant. The COP reached a low of 0.27 to 12.5 hr. Then it increases to a maximum value of 0.58 to 16 hr. Depending on the fixed operative and initial conditions, the average COP of the machine is equal to 0.512. Thus, the overall average yield of the cycle is 0.2. That is to say, we succeeded to transforms 20% of the solar illumination available on the surface of the solar collector in cooling load.

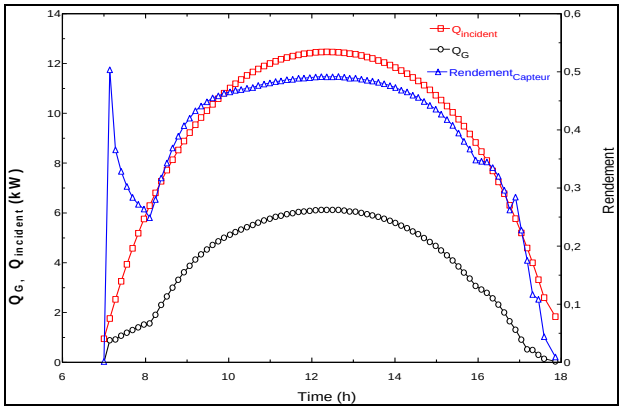

Fig. 8 Instantaneous efficiency of solar collector versus time.

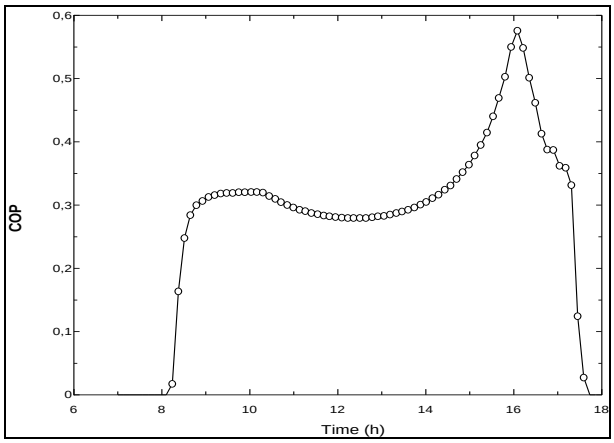

Fig. 9 Instantaneous efficiency of solar collector versus time.

In Fig. 10, is shown the performance of the machine for different initial mass fraction in NH_3. It is noted that the average coefficient of performance increases with increasing of initial mass percentage of the ammonia solution. The COP increases with increasing initial mass fraction up to a certain optimum due to the increase of the mass fraction of rich and poor solutions flows. More than the flow rate of the rich solution contains ammonia more than can evaporate, and therefore the efficiency of the refrigerating machine improves. After this optimum, the COP decreasing continuously due to the inability of the refrigerating machine (approximately from the value of X_{G0} = 0.51) to absorb the entire quantity of ammonia generated as shown in Fig. 11. Thus the evaporator in the period that has the most intense heat flow is filled with the cooling liquid overflows through the full up to the absorber, this overflow does not produce the cooling effect and reduces the efficiency of the machine.

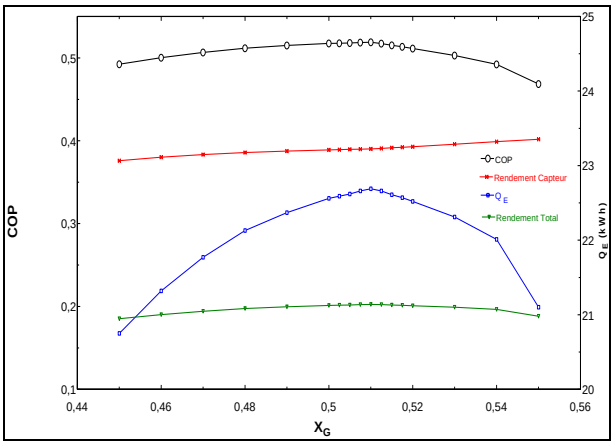

Fig. 10 $\overline{COP}$ and $\overline{Q_E}$ as a function of initial mass percentage.

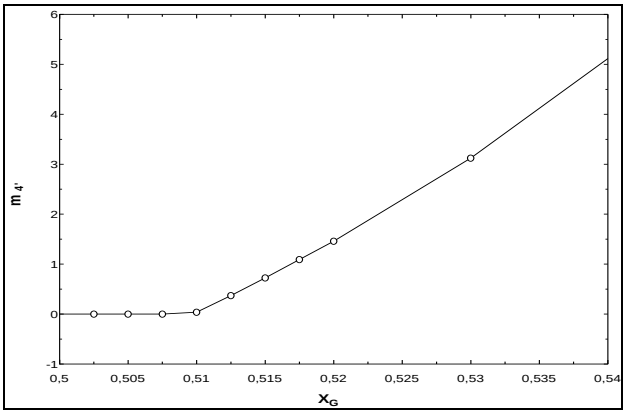

Fig. 11 Level control flow as function of initial mass percentage.

5. Conclusion

The development of the energy and mass balances in every component of the cycle has allowed us to simulate at transient regime the performance of a solar absorption refrigerator operating with NH_3/H_2O. The installation is driven in an autonomous way. Under a sunny day conditions, the machine transforms 20% of

the available solar illumination in cooling load. The machine produces cooling with an almost constant power of about 2 kW. The temperature inside the evaporator is 2°C whereas outside the temperature is set to 5 °C. The developed model could be used to assess the performance of an autonomous intermittent absorption refrigerator.

References

[1] Y. Fan, L. Luo, B. Souyri, Review of solar sorption refrigeration technologies: Development and applications. Renewable and Sustainable Energy Reviews. 11(8), (2007) 1758–1775.

[2] N. A. Darwish, S. H. Al-Hashimi, A. S. Al-Mansoori, Performance analysis and evaluation of a commercial absorption–refrigeration water–ammonia (ARWA) system. International Journal of Refrigeration. 31(7) (2008) 1214-1223.

[3] J.M. Gordon, K.C. Ng, A general thermodynamic model for absorption chiller: theory and experiment. Heat Recovery Systems and CHP. 15(1) 77–83 (1995).

[4] K.C. Ng, et al., Theoretical and experimental analysis of an absorption chiller. International Journal of Refrigeration. 17(5) (1993) 351–358.

[5] G. Grossman, A. Zaltash, ABSIM – modular simulation of advanced absorption systems. International Journal of Refrigeration. 24(6) (2001) 531–543.

[6] M. D. Staicovici, An autonomous solar ammonia–water refrigeration system. Sol Energy. 36 (2) (1986) 115-124.

[7] F. Assilzadeh, S. A. Kalogirou, Alia Y., K.. Sopian, Simulation and optimization of a LiBr solar absorption cooling system with evacuated tube collectors. Renewable Energy. 30 (8) (2005) 1143-1159.

[8] M. Imroz Sohel, B. Dawoud, Dynamic modelling and simulation of a gravity-assisted solution pump of a novel ammonia–water absorption refrigeration unit. Applied Thermal Engineering. 26 (7) (2006) 688–699.

[9] P. Kohlenbach, F. Ziegler, A dynamic simulation model for transient absorption chiller performance, Part I: the model. International Journal of Refrigeration. 31 (2) (2008) 217-225.

[10] P. Kohlenbach, F. Ziegler, A dynamic simulation model for transient absorption chiller performance, Part II: numerical results and experimental verification. International Journal of Refrigeration. 31 (2) (2008) 226-233.

[11] H. Matsushima, T. Fujii, Komatsu T, A. Nishiguchi, Dynamic simulation program with object-oriented formulation for absorption chillers (modelling, verification, and application to triple-effect absorption chiller). International Journal of Refrigeration. 33 (2) (2010) 259-268.

[12] M. Zinet, R. Rulliere, P. Haberschill, A numerical model for the dynamic simulation of a recirculation single-effect absorption chiller. Energy Conversion and Management. 62, (2012) 51–63.

[13] A. Iranmanesh, M.A. Mehrabian, Dynamic simulation of a single-effect LiBr-H2O absorption refrigeration cycle considering the effects of thermal masses. Energy and Buildings. 60, (2013) 47–59.

[14] B. Kim, J. Park, Dynamic simulation of a single-effect ammonia–water absorption chiller. International Journal of Refrigeration. 30 (3) (2007) 535–545.

[15] Y. Shin, et al., Simulation of dynamics and control of a double-effect LiBr–H2O absorption chiller. Applied Thermal Engineering. 29 (13) (2009) 2718–2725.

[16] S.C. Kaushik, S.K. Rao, R. Kumari, Dynamic simulation of an aqua-ammonia absorption cooling system with refrigerant storage. Energy Conversion and Management. 32 (3) (1991) 197-206.

[17] N. Sugano, K. Saito, S. Kawai, N. Nisiyama, R. Honma, H. Wakimizu, Simulation and experimental research of dynamic characteristics of single-effect absorption refrigerators driven by waste hot water. Trans, JSME (B). 60 (576) (1994) 290-296.

[18] E. Willers, M. Groll, C. Kulick, F. Meunier, C. Mostofizadeh, P. Neveu, M. Wierse, Dynamic modeling of a liquid absorption system. ISHPC, Munich, Germany, (1999) 181-185.

[19] Y. Boukhchana, A. Fellah, A. Ben Brahim, Modeling of the Generation Phase of an Intermittent Solar Absorption Refrigeration System: Effects of the Thermal Losses. I.RE.CH.E. 2 (5) (2010) 577-583.

[20] Y. Boukhchana, A. Fellah, A. Ben Brahim, Modélisation de la phase génération d'un cycle de réfrigération par absorption solaire à fonctionnement intermittent. International Journal of Refrigeration. 34 (1) (2011) 159-167.

[21] W. Cai, M. Sen, S. Paolucci, Dynamic modeling of an absorption refrigeration system using ionic liquids, ASME International Mechanical Engineering Congress and Exposition, Seattle, Washington, USA, (2007).

[22] A. Fellah, Intégration de la décomposition hiérarchisée et de l'endoréversibilité dans l'étude d'un cycle de réfrigération par absorption solaire. Thesis in Mechanical Engineering, University of Tunis El Manar, National School of Engineers of Tunis (2008).